

Multifarious Physics Analysis of the Core Plasma Properties in a Helical DEMO Reactor FFHR-d1

J. Miyazawa¹, M. Yokoyama¹, Y. Suzuki², S. Satake², R. Seki², Y. Masaoka², S. Murakami², Y. Narushima², M. Nunami², T. Goto², C. Suzuki², H. Funaba², I. Yamada², R. Sakamoto², G. Motojima², H. Yamada², A. Sagara², and FFHR Design Group

¹National Institute for Fusion Science (NIFS), 322-6 Oroshi, Toki, Gifu 509-5292, Japan

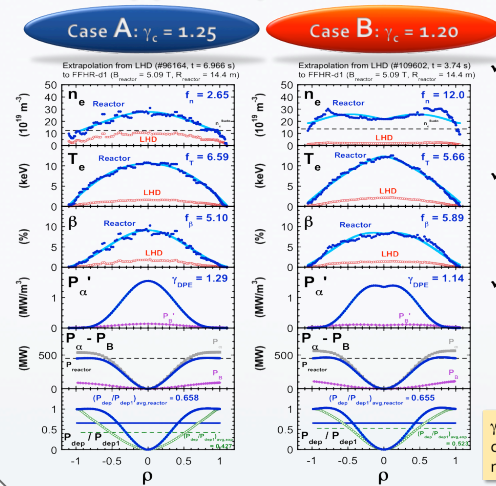
²National Department of Nuclear Engineering, Kyoto University, Kyoto 606-8501, Japan



Summary

- ✓ **Multifarious physics analyses of the core plasma properties in FFHR-d1 have been carried out**
 - Using profiles directly extrapolated from LHD
- ✓ **Large Shafranov shift is foreseen and will cause ...**
 - deterioration in both neoclassical transport and α particle confinement
- ✓ **Promising procedures to deal with this are found:**
 - optimization of the magnetic configuration
 - plasma position control by B_y
- ✓ **Then, it becomes possible to realize:**
 - magnetic surfaces similar to those in vacuum
 - neoclassical transport compatible with α heating
 - small alpha energy loss of ~10 %

Two typical profiles have been chosen



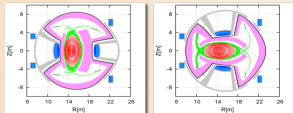
- ✓ One from the standard configuration of $R_{ax} = 3.60$ m, $\gamma_c = 1.25$
- ✓ Another from the high aspect ratio configuration of $R_{ax} = 3.60$ m, $\gamma_c = 1.20$
- ✓ The high-aspect ratio configuration is effective for Shafranov shift mitigation

$\gamma_c = (m a_c) / (l R_c)$ is the pitch of helical coils, where $m = 10$, $l = 2$, $a_c \sim 0.9 - 1.0$ m, and $R_c = 3.9$ m in LHD

Helical DEMO reactor FFHR-d1

A. Sagara et al., Fusion Eng. Des. 87, 594 (2012)

- Conceptual design study of FFHR-d1 has been started in 2010
- The newest version of the FFHR series (FFHR1, FFHR2, FFHR2m1, FFHR2m2)
 - ✓ Heliotron type steady-state reactor
 - ✓ Self-ignition (no auxiliary heating)
 - ✓ 3 GW of fusion output
 - ✓ 1.5 MW/m² of neutron wall load
- What's new in FFHR-d1
 - ✓ Coil arrangement is similar to LHD
 - ✓ Based on LHD normal confinement
 - ✓ $R_c = 15.6$ m (LHD $\times 4$), $B_c = 4.7$ T
 - ✓ 3 pairs of poloidal coils in LHD are reduced to 2 in FFHR-d1, to secure the large ports for maintenance
 - ✓ Divertors are placed on the backside of blankets



Schematic view of FFHR-d1

Vertical slices of FFHR-d1

Attractive features of a helical reactor

Flux surfaces are generated by external superconducting coils

- Plasma current drive is unnecessary
- Steady state operation is easy
- Circulating energy is ~10 % of fusion output
- Plasma does not contact with the blanket at start up / shut down / emergency
- No plasma current disruption

Divertors are placed behind the blankets

- To avoid direct neutron irradiation (both of the neutron damage and radioactivation can be reduced)
- Divertor detachment becomes easy



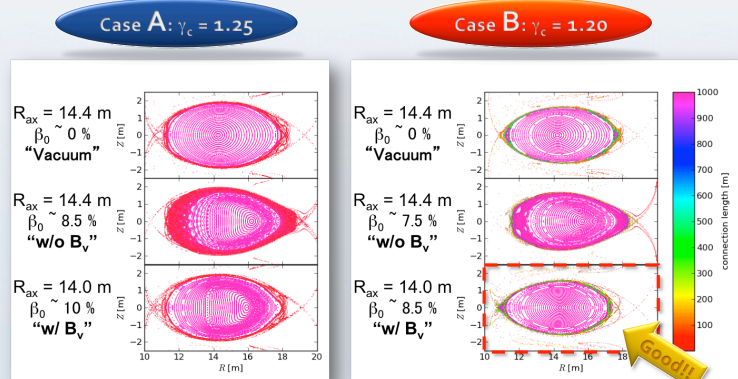
Open space inside the torus

- No needs of center solenoid

Neutron wall load can be reduced by enlarging the device size

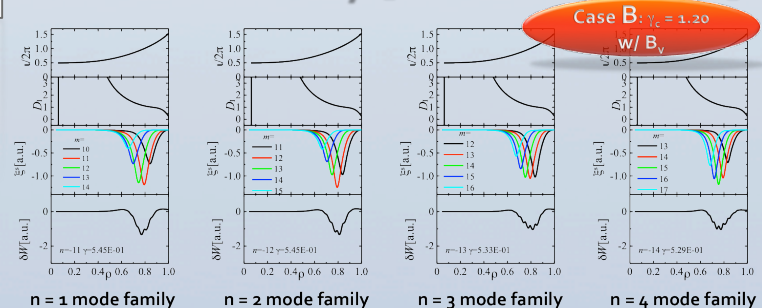
- No need of non-inductive current drive of which the needed power is proportional to the device size
- Long-life blanket
- Low decay heat

MHD Equilibrium [HINT2]



- ✓ Shafranov shift can be mitigated and destructed magnetic surfaces are reformed by plasma position control using vertical magnetic field
- ✓ Especially, magnetic surfaces similar to those in vacuum are formed with finite beta in the high aspect ratio configuration

MHD Stability [TERPSICHORE]

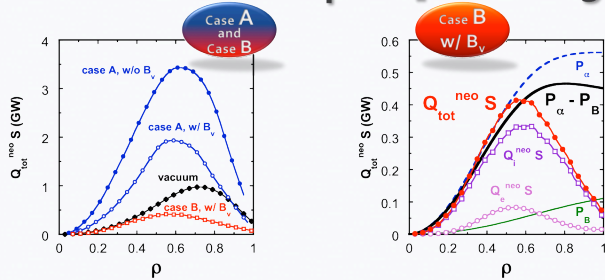


- ✓ Inward-shifted configurations are Mercier unstable
- ✓ High mode number MHD instabilities are foreseen at iota ~ 1, instead of low mode number MHD

Description on applied numerical codes

Physics Topics	Code	Functions and Remarks	Responsible Person
3D Equilibrium	VMEC	3d equilibrium is calculated inside the last closed flux surface (provided by HINT2). Closed flux surfaces are a priori assumed.	R. Seki
	HINT2	→ Equilibrium Database	
MHD stability	TERPSICHORE	3d equilibrium is calculated WITHOUT assuming closed flux surfaces (stochastic field, magnetic islands, can be treated) → field data to MORH	Y. Narushima
Neoclassical diffusion/ ambipolar Er	FORTEC-3D	Drift kinetic equation is solved based on δf Monte-Carlo approach. Finite orbit width effect is rigorously treated. "Global" neoclassical diffusion (and then ambipolar radial electric field, Er) and viscosities are evaluated.	S. Satake
	GSRAKE	Bounce-averaged drift kinetic equation is solved to evaluate "local" neoclassical diffusion (and then ambipolar Er). Computations time is relatively short, however, accuracy becomes worse in magnetic configurations with broader spectrum (such as high-beta regime).	S. Satake
α particles confinement	GNET	Drift kinetic equation is solved in 5-dimensional space (geometry, velocity) based on orbit-following approach to obtain the steady-state distribution of energetic particles.	Y. Masaoka/ S. Murakami (Kyoto Univ.)
	MORH	→ α particles confinement, plasma heating	
Turbulent transport	GKV-X	Energetic particles' orbit following using the magnetic field data provided by HINT2. Re-entering particles are also taken into account.	R. Seki
		Turbulent transport analysis based on solving the time-evolution of the ions' and electrons' fluctuation distribution function in 5d space based on gyro-kinetic equation.	M. Nunami
		→ ITG turbulence, zonal flow issues etc.	

Neoclassical Transport [FORTEC3D]



Neoclassical heat flow in various cases Comparison with P_α in Case B w/ B_v

- ✓ Large neoclassical transport is expected in the case A w/o B_v
- ✓ Plasma position control with B_v is effective and the heat flux is halved
- ✓ Neoclassical heat flux in the Case B with B_v is smaller than the alpha heating power minus the radiation loss of ~ 400 MW at $\rho > 0.6$

→ Both high aspect ratio config. and plasma position control is effective

Alpha Particle Confinement [GNET]

- ✓ Heat deposition profile is peaked
Case A w/ B_v : $(P_{dep}/P_{dep1})_{avg} \sim 0.65$ (B_v effect is unclear)
Case B w/ B_v : $(P_{dep}/P_{dep1})_{avg} \sim 0.51$
- ✓ Significant loss of alpha particle due to the large Shafranov shift

Energy loss ratio:

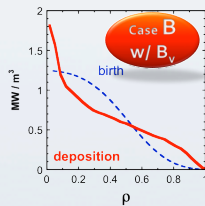
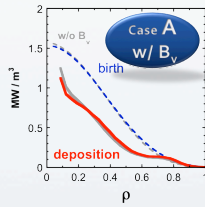
Case A w/ B_v : 41 % → Case B w/ B_v : 11 %

Particle loss ratio:

Case A w/ B_v : 69 % → Case B w/ B_v : 20 %

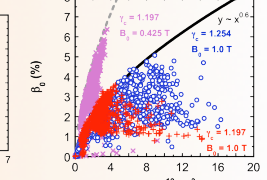
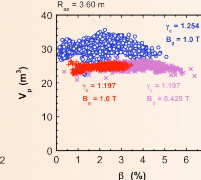
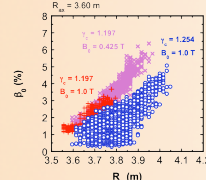
Note: Reentering alpha is not considered

(α particles are lost at LCFS in GNET)



High aspect ratio configuration can be a strong option $\gamma_c = 1.20$

- ✓ Shafranov shift is drastically mitigated
- ✓ The blanket space can be enlarged
- ✓ The effective plasma volume, V_{pr} is relatively small
- ✓ Similar performance with the standard configuration in spite of the smaller V_p



3D Tracking of Alpha Particles [MORH]

- ✓ Three dimensional orbit tracing by MORH using MHD equilibriums given by HINT2

- $E_\alpha = 3.5$ MeV

- $\rho = 0.1 - 0.9$

- $\phi = 0^\circ - 18^\circ$

- pitch angle = $(1 - 19) \pi/20$

- w/o CX loss

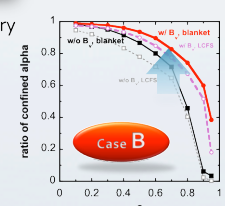
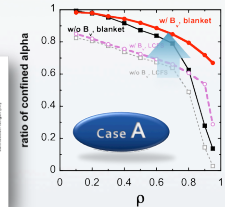
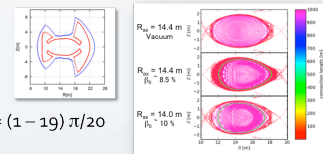
- Vacuum vessel or blanket is used as the loss boundary

(no significant difference is recognized)

- ✓ Plasma position control is effective

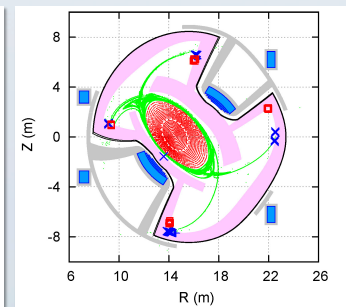
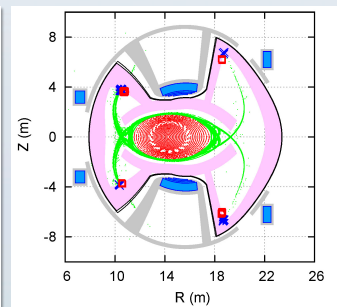
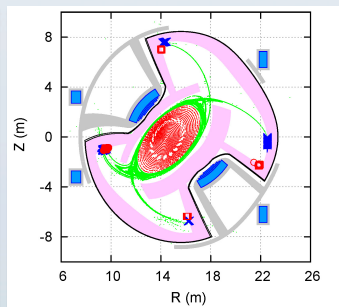
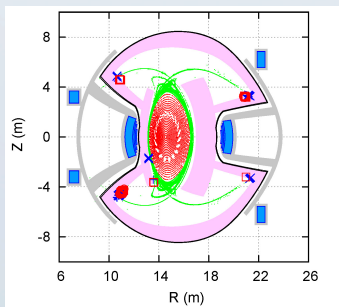
- ✓ Reentering effect is also effective

- ✓ Direct loss of alpha particles generated at $\rho < 0.7$ is less than 20 %



Alpha Particles Go To the Divertor Region [MORH]

Case A (x: w/o B_v , +: w/ B_v) and Case B (□: w/o B_v , ○: w/ B_v)



- ✓ Basically, the major part of the lost α particles goes to the divertor region behind the blanket in FFHR-d1
- ✓ Negligibly small number of lost α particles starting from $\rho = 0.95$ hit the blanket side wall

Direct Profile Extrapolation (DPE)

J. Miyazawa et al., Fusion Eng. Des. 86, 2879 (2011)

- ✓ Directly extrapolates the profile data to reactor
- ✓ Extrapolation without assumed profiles
- ✓ MHD equilibrium similar to the experiment is used
- ✓ Gyro-Bohm normalized pressure profile is fixed

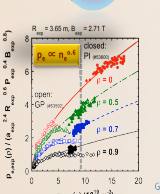
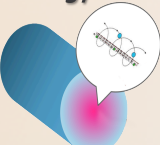
$$P_{GB-BPM}(p) = \alpha_p n_p(p)^{0.5} p_{0.4} B^{0.8} j_{\perp}(2.4 p / \alpha_p)$$

- ✓ Enhancement factors of beta and density are determined to achieve self-ignition

- ✓ The heating profile effect is also taken into account

$$\begin{aligned} T_{reactor}(p) &= f_T T_{exp}(p) & R_{reactor} &= f_R R_{exp} \\ n_{reactor}(p) &= f_n n_{exp}(p) & B_{reactor} &= f_B B_{exp} \\ a_{reactor} &= f_a a_{exp} & P_{reactor} &= f_P P_{exp} \\ f_T &= f_B f_n^{-1} f_a^{-1} & & \\ f_P &= f_B f_n^{-2.5} f_a^{-2.5} f_T^{-1.5} & \leftarrow \text{Gyro-Bohm} \\ f_B^2 &= f_P P_{exp} / (f_T^2 \int_0^1 (P_\alpha - P_\beta) (dV/d\rho)_{exp} d\rho) \end{aligned}$$

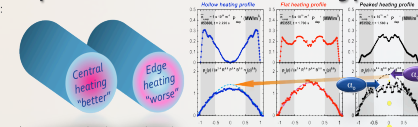
Energy confinement is gyro-Bohm



- Scale length of the turbulence - ion gyro radius: $\lambda_i \propto \rho_i \propto T^{1/2}/B$
- Time scale of the turbulence - (ion diamagnetic drift frequency) $^{-1}$: $\tau \propto \omega_p^{-1} \propto (1/\rho_i)(\rho_i/a)^{-1} T^{3/2}$
- Bohm diffusion coefficient: $D_B \propto T/B$
- Gyro-Bohm diffusion coefficient: $D_{GB} \propto \lambda_i^2/\tau \propto \rho_i^2 \omega_p^{-1} \propto T^{-3/2}/(aB^2)$
- Gyro-Bohm type energy confinement time scaling: $\tau_{GB} \propto a^{1/2} R^{3/2} P^{-3/5} n^{3/5} B^{4/5}$
- ISS95 and ISS04, H-mode scaling

Gyro-Bohm type dependence of the local pressure on the local density

The confinement enhancement factor is expressed as a function of the heating profile



- ✓ Regression analysis between the peaking factor of the heating profile and the confinement enhancement factor
- ✓ $\alpha_p \propto (P_{exp}/P_{exp1})^{0.44}$ P_{exp1} is the fitting result for $0.5 < p < 1$
- ✓ $\alpha_p \propto (P_{exp}/P_{exp1})^{0.44}$ P_{exp1} is the fitting result for $0.5 < p < 1$
- ✓ Confinement enhancement factor $\alpha_p \propto (P_{exp}/P_{exp1})^{0.44}$

Over 800 time slices are extracted from 50 discharges in the LHD 8T campaign in 2006

$$\gamma_{DPE} \propto (P_{exp}/P_{exp1})_{avg, reactor} / (P_{exp}/P_{exp1})_{avg, exp}^{0.6} = (0.65 / (P_{exp}/P_{exp1})_{avg})^{0.6}$$